Expanded View Figures

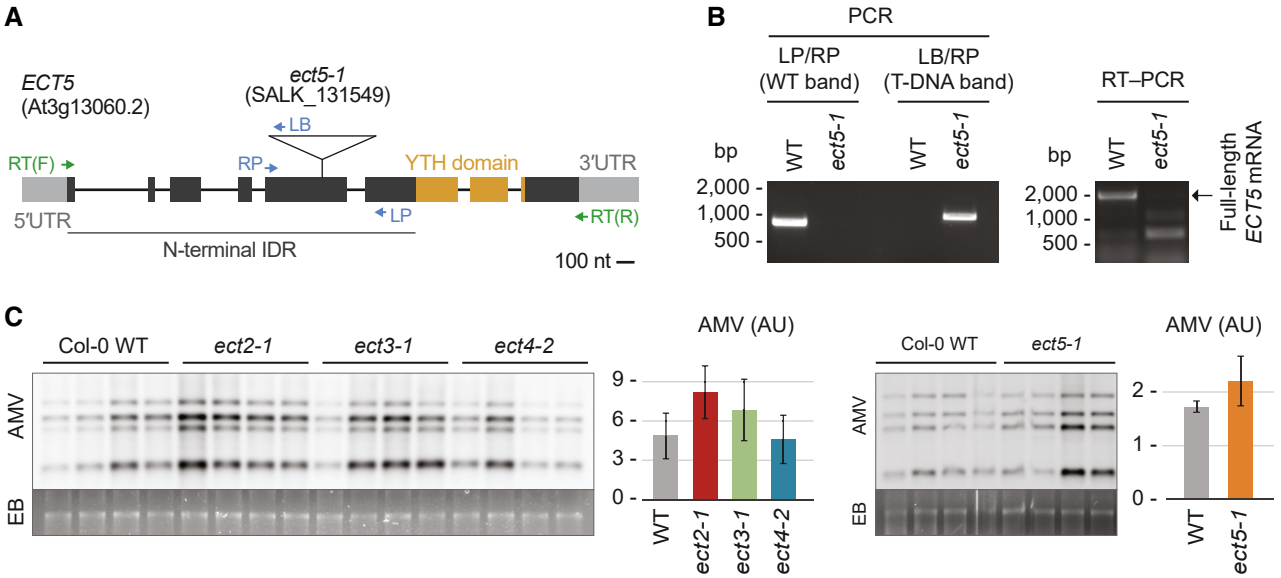

Figure EV1. Single mutation of *ECT2*, *3*, *4*, or *5* alone does not alter AMV infection.

A *ECT5* gene model (AT3G13060.2) showing the location of the *ect5-1* T-DNA insertion (SALK_131549, Appendix Table S1). Exons are depicted as boxes and introns as lines. Untranslated regions (UTRs) are colored in light gray, and the exonic regions encoding the YTH domain are highlighted in light brown. Position of the primers used to amplify full-length *ECT5* are depicted in green, and genotyping primers in blue.

B Ethidium bromide-stained agarose gels showing *ect5-1* genotyping by PCR (left panel) to corroborate the presence of the T-DNA, and RT-PCR (right panel) to amplify the full-length transcript. Location of primers LP (left primer, genomic), RP (right primer, genomic), and LB (left border primer, T-DNA) are schematically shown in blue (A), whereas nucleotide sequences can be found in Appendix Table S2.

C RNA-blot analysis of AMV systemic infection at 7 days postinoculation *ect2-1*, *ect3-1*, *ect4-2* (left panels), and *ect5-1* (right panels) mutants compared with wild-type plants. Each panel shows a representative RNA blot displaying AMV RNAs 1–4 (left) and its quantification histogram (right). Ethidium bromide staining of rRNAs (EB) was used as RNA loading control. Error bars indicate standard deviation and the Student's *t*-test ($n = 4$) was applied. AU, arbitrary units.

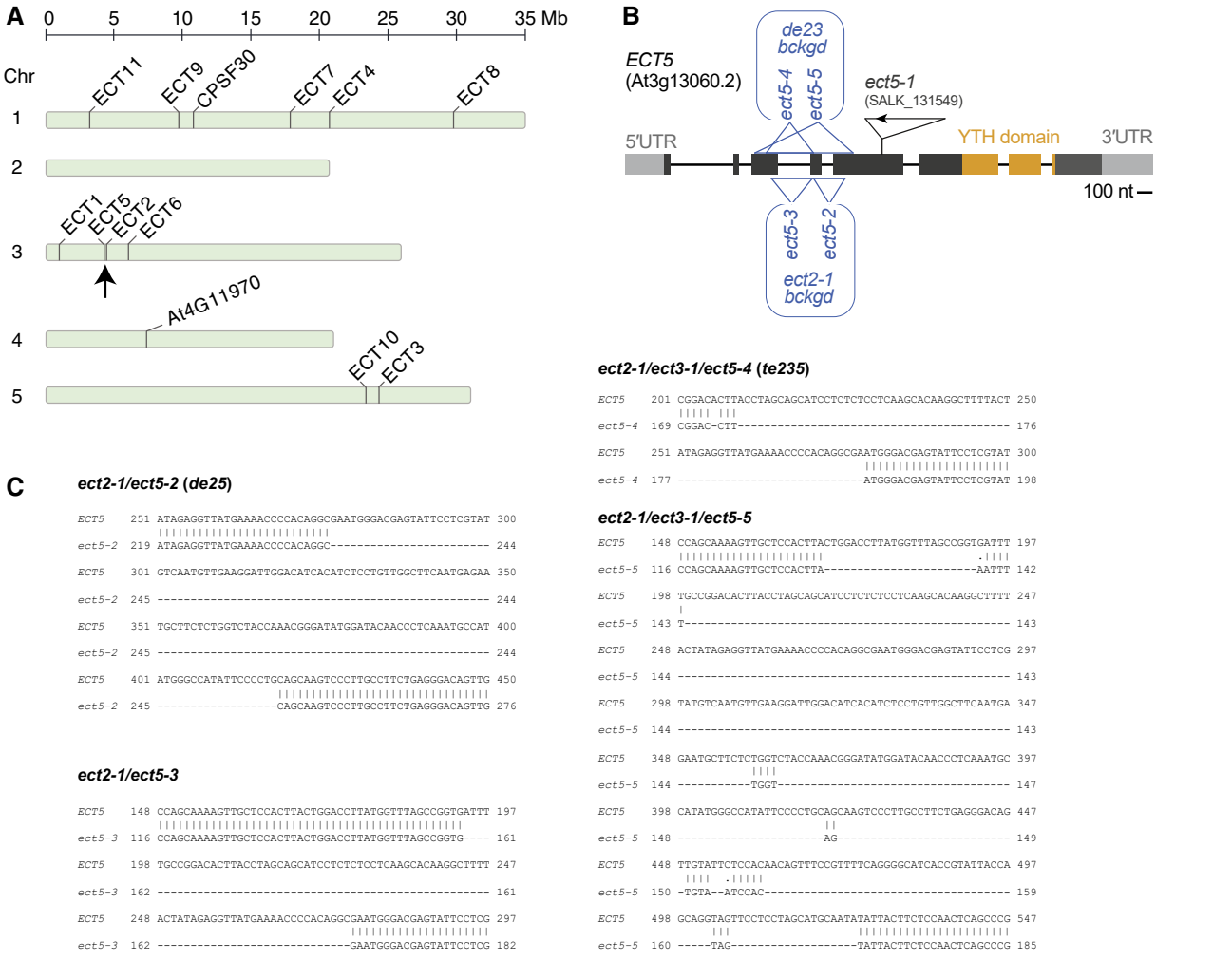

Figure EV2. *ECT5* CRISPR/Cas9 mutants on the *ect2-1 and de23 backgrounds.*

A Schematic map of the five nuclear chromosomes (Chr 1–5) of *Arabidopsis thaliana*. The position of the 13 genes encoding YTH domain proteins (11 YTHDFs (ECTs) and two YTHDCs (CPSF30 and AT4G11970)) is indicated. A black arrow marks the positions of ECT2 and ECT5 loci, in close proximity. Mb, megabase pairs.

B Schematic representations of the annotated ECT5 gene (AT3G13060.2) showing the location of the ect5-1 T-DNA insertion (SALK_131549) and, marked in blue, the four deletions engineered using CRISPR/Cas9 in the *ect2-1* (*ect5-2* and *ect5-3*) or *de23* (*ect5-4* and *ect5-5*) backgrounds. Exons are depicted as boxes and introns as lines. Untranslated regions (UTRs) are colored in light gray, and the exonic regions encoding the YTH domain are highlighted in light brown.

C Alignment between the Sanger-sequencing reads obtained from cDNA of the four CRISPR/Cas9 alleles described in (B), and wild-type ECT5 cDNA (AT3G13060.2) showing the deletions produced by Cas9.

D Alignment between the amino acid sequences of wild-type ECT5 and the proteins predicted to be encoded by the Cas9-edited *ECT5* loci described in (B and C). The four deletions cause shifts in the ORF that result in short amino acid stretches (marked in red) that end with a premature stop codon (*).

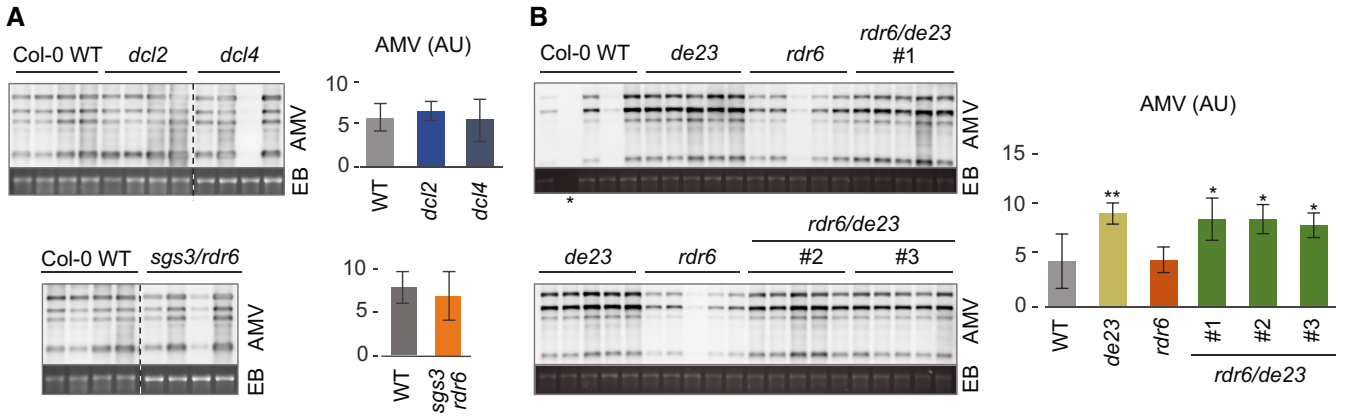

Figure EV3. Effect of the RNAi antiviral pathway in AMV infection.

A, B AMV systemic infection at 7 days postinoculation in *dcl2*, *dcl4*, and *sgs3/rdr6* (A) or in *rdr6/de23* lines (B) compared with wild-type (WT). Each panel shows a representative RNA blot displaying AMV RNAs 1–4 (left) and its quantification histogram (right). Genotypes are indicated on the top of each northern blot. #1, #2, and #3 correspond to the progeny of three different triple homozygous F2 siblings derived from the *rdr6* x *de23* cross. Ethidium bromide staining of rRNAs (EB) was used as RNA loading control. Error bars indicate standard deviation, and asterisks indicate significant differences from the WT (**: $P < 0.01$) applying the Student's *t*-test. AU, arbitrary units. *, lane excluded from the statistical analysis (in B, upper panel).

Source data are available online for this figure.

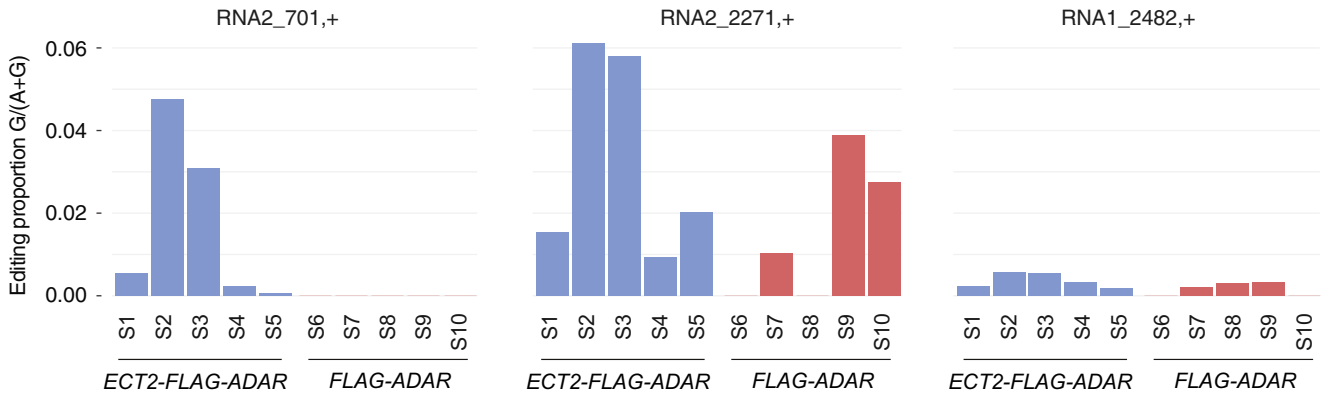

Figure EV4. Editing proportions (G/(A + G)) for the top three most significant positions in AMV RNAs in individual samples.

Histograms showing the editing proportions (A-to-G) of the three top positions in AMV RNAs identified by HyperTRIBE pipeline over five independent transgenic lines of ECT2-FLAG-ADAR and FLAG-ADAR control lines.

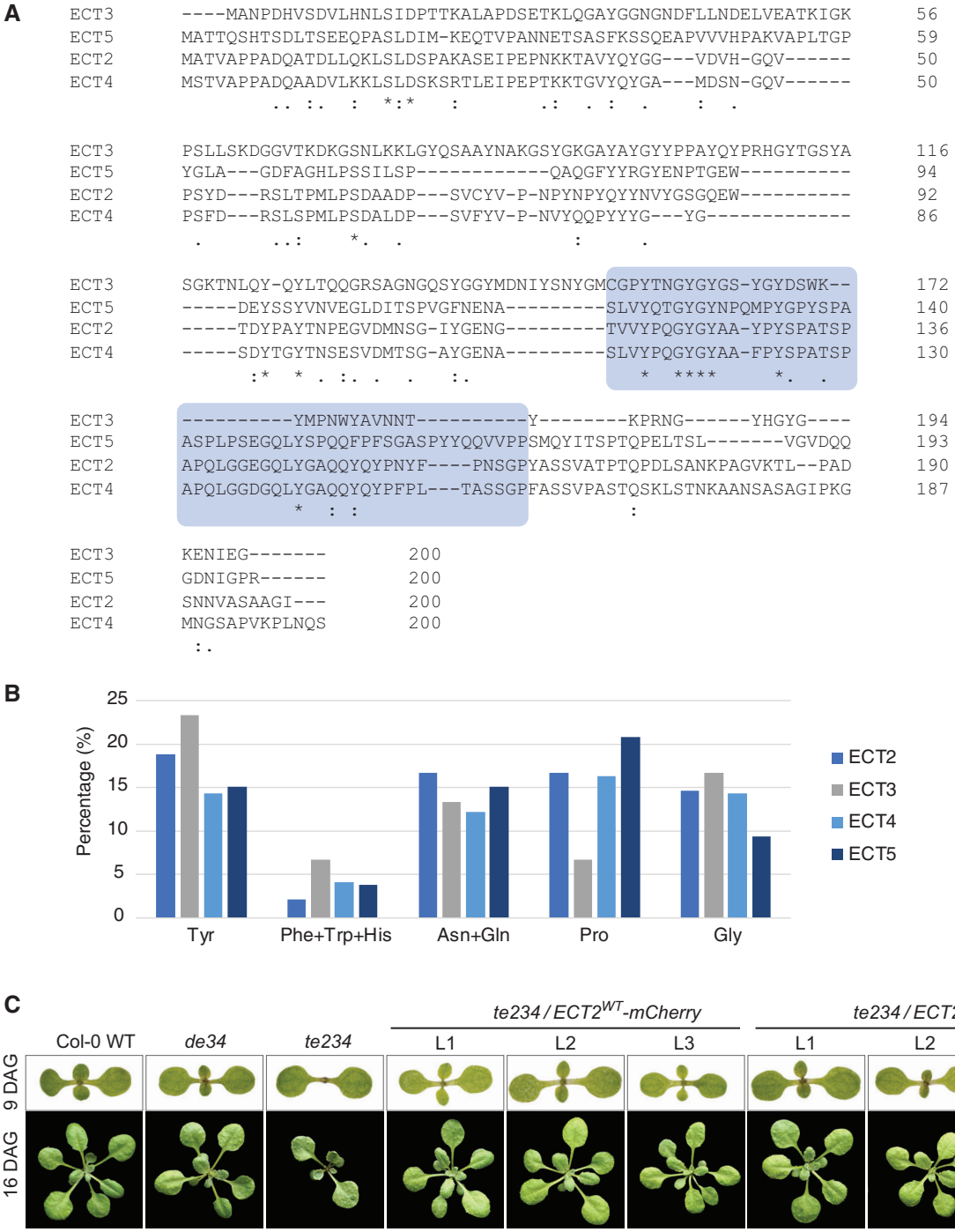

Figure EV5. Analysis of ECT2$^{\Delta N5}$-mCherry mutants.

A Tyr-rich region deleted in ECT2$^{\Delta N5}$-mCh mutants is conserved to some extent in ECT3, 4, and 5 (shaded in blue). Multiple sequence alignment of the N-terminal 200 amino acid region of these proteins (Clustal Omega).

B Amino acids proportion (%) of ECT2, 3, 4, and 5 in the section that aligned with the Tyr-rich region.

C Full complementation of the developmental phenotype of *te234* mutants by expression of ECT2$^{\Delta N5}$-mCherry is comparable to that of wild-type ECT2^{WT}-mCherry, as seen in three independent lines of each type (used for the infection assays in Fig 6B) compared with WT or *de34* plants. DAG, days after germination. Scale bars are 1 mm for the upper panels, and 1 cm for the lower.